The two processes should lead to anisotropic conductivity along and perpendicular to the *c* direction, an effect which has already received experimental confirmation (Baranov, 1989). The structural results indicate no possiblity of the Cs^+ diffusion as reported elsewhere (Pham-Thi, Colomban, Novak & Blinc, 1987). Haynovskiy, Pavlyuhin & Hayretdinov (1985) reported that in the low-temperature phase the conductivity of $CsHSO_4$ is two orders of magnitude higher than that of $CsDSO_4$, whilst in the superionic phase their conductivities are approximately equal. From this arose the assumption that the diffusion of Cs^+ contributes to the conductivity (Pham-Thi, Colomban, Novak & Blinc, 1987). However as noted above the room-temperature structure of $CsHSO_4$ differs from that of $CsDSO_4$ and so the large difference in conductivity in the low-temperature phases of protonated and deuterated samples cannot be solely assigned to an isotopic effect as previously stated (Haynovskiy, Pavlyuhin & Hayretdinov, 1985).

The authors wish to express their gratitude to Mrs N. M. Shchagina for preparing the sample and Z. Jirak for valuable discussions and suggestions during the data analysis. One of us (AVB) would like to acknowledge the SERC and the RAL directorate for access to the ISIS facilities and for financial support.

References

Balagurov, A. M., Belushkin, A. V. & Beskrovnyi, A. I. (1985). *JINR Rapid Commun. Dubna*, pp. 13–85.

Balagurov, A. M., Beskrovnyi, A. I. & Savenko, B. N. (1987). *Phys. Status Solidi A*, **100**, K3–10.

Baranov, A. I. (1989). *Solid State Ionics*, **36**, 279–282.

Baranov, A. I., Shuvalov, L. A., Fedosyuk, R. M. & Schagina, N. M. (1984). *Ferroelectrics Lett.* **2**, 25–28.

Baranov, A. I., Shuvalov, L. A. & Schagina, N. M. (1982). *Pis'ma Zh. Eksp. Teor. Fiz. (USSR)*, **36**, 381–384; *JETP Lett.* **36**, 459.

Baranov, A. I., Shuvalov, L. A. & Schagina, N. M. (1984). *Kristallografiya*, **29**, 1203–1205; *Sov. Phys. Crystallogr.* **29**, 706.

Belushkin, A. V., Natkaniec, I., Plakida, N. M., Shuvalov, L. A. & Wasicki, J. (1987). *J. Phys.* C, **20**, 671–687.

Blinc, R. (1984). *Phys. Status Solidi B*, **123**, K83–87.

Brown, P. J. & Matthewman, J. C. (1987). Report RAL-87-101. Rutherford Appleton Laboratory, Chilton, Didcot, Oxon, England.

David, W. I. F., Akporiaye, D. E., Ibberson, R. M. & Wilson, C. C. (1988). Report RAL-88-103. Rutherford Appleton Laboratory, Chilton, Didcot, Oxon, England.

Dmitriev, V. P., Loshkarev, V. V., Rabkin, L. M., Shuvalov, L. A. & Yuzyuk, Yu. I. (1986). *Kristallografiya*, **31**, 1138–1145.

Haynovskiy, N. M., Pavlyuhin, Yu. T. & Hayretdinov, E. F. (1985). *Izv. Sib. Otd. Acad Nauk SSSR Ser. Khim. Nauk (USSR)*, **11**, 99–107.

Jirak, Z., Dlouha, M. & Vratislav, S. (1987). *Phys. Status Solidi A*, **100**, K117–123.

Komukae, M., Osaka, T., Makita, Y., Ozaki, T., Itoh, K. & Nakamura, E. (1981). *J. Phys. Soc. Jpn.* **50**, 3187–3188.

Merinov, B. V., Baranov, A. I., Maksimov, B. A. & Shuvalov, L. A. (1986). *Kristallografiya*, **31**, 450–454; *Sov. Phys. Crystallogr.* **31**, 264.

Merinov, B. V., Baranov, A. I., Shuvalov, L. A. & Maksimov, B. A. (1987). *Kristallografiya*, **32**, 86–94; *Sov. Phys. Crystallogr.* **32**, 47.

Pham-Thi, M., Colomban, Ph., Novak, A. & Blinc, R. (1985). *Solid State Commun.* **55**, 265–270.

Pham-Thi, M., Colomban, Ph., Novak, A. & Blinc, R. (1987). *J. Raman Spectrosc.* **18**, 185–190.

Yokota, S. (1982). *J. Phys. Soc. Jpn*, **51**, 1884–1891.

Acta Cryst. (1991). B**47**, 166–174

A Modulation-Wave Approach to the Structural Description of the $Nb_2Zr_{x-2}O_{2x+1}$ (x = 7·1–10·3) Solid-Solution Field

By R. L. Withers, J. G. Thompson and B. G. Hyde

Research School of Chemistry, Australian National University, GPO Box 4, *Canberra, ACT* 2601, *Australia*

(*Received* 22 *June* 1990; *accepted* 24 *September* 1990)

Abstract

At the ZrO_2-rich end of the phase diagram, the $Nb_2O_5 + ZrO_2$ system forms a complex $Nb_2Zr_{x-2}O_{2x+1}$ (x = 7·1–10·3) solid-solution field which can be structurally characterized as a composite modulated structure. Fourier decomposition of the Galy & Roth [*J. Solid State Chem.* (1973), **7**, 277–285] structure refinement of one composition within this field, *i.e.* $Nb_2Zr_6O_{17}$, in such terms gives the underlying parent metal-atom subcell (*Amma*, $a_M \simeq 5{\cdot}1$, $b_M \simeq 4{\cdot}9$, $c_M \simeq 5{\cdot}2$ Å) and parent O-atom subcell {*Imam*, $a_O = [x/(2x+1)]a_M$, $b_O = b_M$, $c_O = c_M$} along with specific expressions for the atomic modulation functions describing the structural deviation of the two sublattices from their respective parent subcells. The extinction conditions characteristic of this $Nb_2Zr_{x-2}O_{2x+1}$ (x = 7·1–10·3) solid-solution

0108-7681/91/020166-09$03.00

field imply a superspace-group symmetry of M:*Amma*: $-1s1$. This superspace group is defined by the above parent metal-atom subcell in conjunction with the modulation wavevector $\mathbf{q} = \mathbf{b}^*_M + (1/x)\mathbf{a}^*_M$. For $x = 8$, this effectively cuts the number of free structural parameters to be refined in half, *i.e.* certain parameters allowed by the conventional superstructure refinement of Galy & Roth should be constrained to be zero. A modulated-structure approach provides the only possible coherent means of describing this material across the whole of its solid-solution field. Refinements using this approach are clearly needed.

1. Introduction

At the ZrO_2-rich end of the phase diagram, the $Nb_2O_5 + ZrO_2$ system forms a complex $Nb_2Zr_{x-2}O_{2x+1}$ solid-solution field which may be regarded as a stabilized anion-excess zirconia. Recent work has shown that the phase width of this field is $5{\cdot}1 < ZrO_2{:}Nb_2O_5 < 8{\cdot}3$, *i.e.* $7{\cdot}1 < x < 10{\cdot}3$. It was previously thought to be an homologous series M_nO_{2n+2} with $n = 2x$ and M a metal (Roth, Waring, Brouwer & Parker, 1972) but it is now recognized that it is more correctly described as a so-called type II, or composite modulated structure (Janner & Janssen, 1980; Thompson, Withers, Sellar, Barlow & Hyde, 1990). Reciprocal space is dominated by a conspicious set of strong matrix reflections $\mathbf{G} = (h,k,l)^*_M$ corresponding to a metrically orthorhombic average metal subcell (*Amma*, $a_M \simeq 5{\cdot}1$, $b_M \simeq 4{\cdot}9$, $c_M \simeq 5{\cdot}2$ Å). A rather weaker set of incommensurate satellite reflections occur at $\mathbf{G} \pm m\mathbf{q} = (h,k,l,m)^*$, where m is an integer, and with $\mathbf{q} \simeq (1/x)\mathbf{a}^*_M + \mathbf{b}^*_M$ (de Wolff, 1974).

Given the experimental observation of a continuous smooth variation of $\mathbf{q}$ across the whole solid-solution field (*i.e.* the lack of any evidence for $1/x$ 'locking in' to a rational fractional such as $\frac{1}{8}$, $\frac{2}{17}$, $\frac{1}{9}$...), it is clear that a generally applicable crystallographic description of this phase must be based upon a modulated-structure, or superspace-group, approach rather than upon conventional crystallographic structure refinement at rational values of $1/x$. In general $\mathbf{q}$ is incommensurable with $\mathbf{G}$. For rational values of x, however, it appears that a superstructure approximation can be made and a conventional three-dimensional structure refinement carried out. Only one such structure refinement has ever been made within this solid-solution field and that was for $Nb_2Zr_6O_{17}$, *i.e.* for $x = 8$ (Galy & Roth, 1973). The purpose of this paper is to Fourier decompose this crystal structure refinement into its two constituent modulated structures – one corresponding to the metal sublattice and the other to the oxygen sublattice. Both these metal and oxygen sublattices possess well-defined underlying parent subcells which it is reasonable to presume remain fairly constant across the whole solid-solution field. The interaction of these two, in general, mutually incommensurable parent subcells leads to modulation (again, in general, incommensurate) of both (de Wolff, 1988). Fourier decomposition of the Galy & Roth (1973) structure solution in terms of these parent subcells and their accompanying displacive modulations enables a picture to be built up of the whole solid-solution field provided we make the reasonable assumption that only the modulation wavevectors, and not the corresponding displacement eigenvectors, vary substantially across the solid-solution field. In addition, such a Fourier decomposition enables an interesting comparison to be made of the relative virtues of refining such superstructures *via* a conventional, as opposed to a modulation-wave or superspace-group, approach.

2. The underlying parent subcells

Most ternary oxides $ZrO_2{:}MO_x$ in which ZrO_2 is the major component have a fluorite-related structure *e.g.* anion-deficient fluorites where M = Mg, Ca, Ln. Thus, when M = Nb or Ta, one might also expect that the parent structure should be fluorite-related, *i.e.* possess an *Fmmm* parent metal-atom subcell with $a_M \simeq b_M \simeq c_M \simeq 5{\cdot}1$ Å and a *Pmmm* parent O-atom subcell with $a_O \simeq b_O \simeq c_O \simeq 2{\cdot}5$ Å. The stoichiometry of the $(Nb,Zr)_xO_{2x+1}$ solid-solution field, however, implies that the average O-atom subcell must be compressed relative to the average metal-atom subcell such that $2x + 1$ oxygen subcells must fit into every x metal subcells.

2.1. *The parent metal-atom subcell*

The conspicuous strong set of matrix reflections $\mathbf{G}$ (see Fig. 1) clearly define the average metal-atom subcell as metrically orthorhombic with $a_M \simeq 5{\cdot}1$, $b_M \simeq 4{\cdot}9$ and $c_M \simeq 5{\cdot}2$ Å. Galy & Roth (1973), for $x = 8$, report a space-group symmetry of *Ima*2 with $a = 40{\cdot}91$, $b = 4{\cdot}93$, $c = 5{\cdot}27$ Å. Appropriate folding back of this structure solution gives an *Amma*, $a_M = 5{\cdot}11$, $b_M = 4{\cdot}93$, $c_M = 5{\cdot}27$ Å averaged metal-atom subcell (with the a glide located at $z = 0{\cdot}0484$) and an *Imam*, $a_O = [x/(2x + 1)]a_M = \frac{8}{17}a_M$, $b_O = b_M$, $c_O = c_M$ averaged O-atom subcell (with the $--m$ plane located at $z = \frac{1}{4} + 0{\cdot}0565$). However the extinction conditions characteristic of the whole solid-solution series (given in §3.2 below), and in particular the condition that $F(h,k,0,m)^*_M = 0$ unless $h = 2n$ (see Fig. 1*d*), require the parent structures of *both* the metal and O-atom subcells to have a least *-mm* point-group symmetry with respect to the same origin. This is consistent with an underlying parent metal-atom subcell sym-

metry of *Amma* but not with *Amm*2. The choice of an underlying parent subcell symmetry is somewhat complicated by the fact that the two subcells are in fact mutually commensurable for $x = 8$, albeit at a high order of commensurability. Thus high-order harmonic $\mathbf{q} \equiv 0$ displacive modulations of each of the underlying parent subcells due to their interaction with the other subcell and resulting in a lowered average structure space-group symmetry are allowed [see §2 of Pérez-Mato, Madariaga, Zuñiga & Garcia Arribas (1987)]. In particular, such $\mathbf{q} \equiv 0$ modes allow an origin shift along the **c** axis for both the parent metal- and O-atom subcells which need not be equal (see §3.3 and 3.4 below). Thus the choice of origin along the **c** direction is somewhat ambiguous. Galy & Roth chose to fix the z coordinates of a specific metal atom at $\frac{1}{2}$. We have chosen to subtract a global origin shift of $0{\cdot}0484\mathbf{c}_M$ from the coordinates of all the Galy–Roth atom positions such that the average, as well as the parent, metal-atom subcell contains an a glide perpendicular to $\mathbf{c}_M$ located at $z = 0$, as required by the observed extinction conditions and as shown in Fig. 2(*a*). Note that the space-group symmetry of the metal-atom subcell would be *Fmmm* and the fractional coordinates identical to those in the related fluorite structure if the parameter δ were zero. In reality, however, the parameter $\delta = 0{\cdot}0394 \simeq 0{\cdot}22$ Å (according to Galy & Roth) and the resultant average (and also parent) metal-atom space-group symmetry *Amma*. Allowed metal-atom subcell reflections include $(200)^*_M$, $(020)^*_M$, $(002)^*_M$, $(011)^*_M$, $(111)^*_M$... .

2.2. *The parent O-atom subcell*

With the above choice of origin, folding back of the Galy & Roth (1973) structure solution gives an *Ima*2, $a_O = [x/(2x+1)]a_M = \frac{8}{17}a_M$, $b_O = b_M$, $c_O = c_M$ averaged O-atom subcell as shown in Fig. 2(*b*). Note that the space-group symmetry would be *Cmmm* (with a halved $\mathbf{c}_O$ axis) if the parameters $\delta_1 = 0{\cdot}0233$ and $\delta_2 = 0{\cdot}0081$ were both zero, and *Imam* if just the small parameter δ_2 was zero. The extinction conditions characteristic of the whole solid-solution series (given in §3.2 below; and see Fig. 1) require the parent structures of both the metal and oxygen

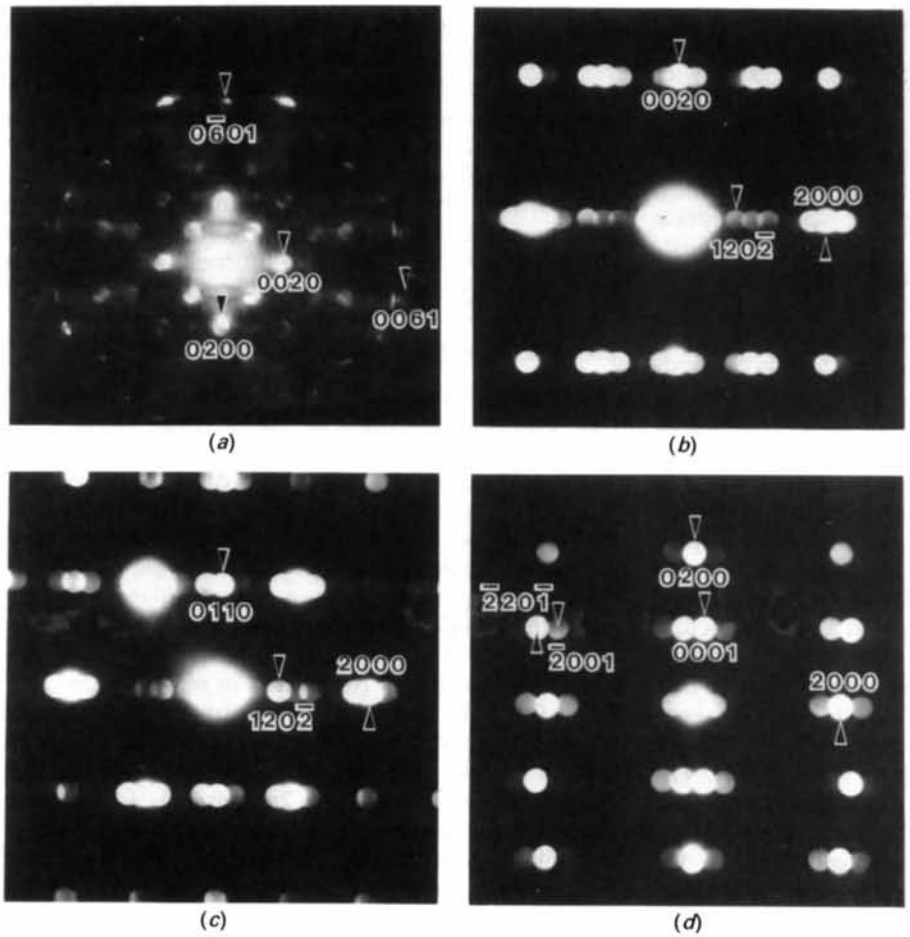

Fig. 1. (*a*) $[100]_M$, (*b*) $[010]_M$, (*c*) $[0\bar{1}1]_M$ and (*d*) $[001]_M$ zone-axis convergent beam diffraction patterns typical of $Nb_2Zr_{x-2}O_{2x+1}$ ($x = 7{\cdot}1$–$10{\cdot}3$). The four-index scheme used for labelling reflections is described in the text.

subcells to have at least *-mm* point group symmetry, consistent with an underlying average oxygen subcell symmetry of either *Cmmm* or *Imam* but not with *Ima*2. The choice of an underlying parent O-atom subcell symmetry is again complicated by the fact that a high-order harmonic $\mathbf{q} \equiv 0$ displacive modulation of the underlying parent oxygen subcell (due to its interaction with the metal subcell), resulting in a lowered average structure space-group symmetry, is allowed [see §2 of Pérez-Mato *et al.* (1987)]. In what follows, we will set δ_2 equal to zero and take the resultant *Imam* structure as the underlying parent O-atom subcell (see Fig. 2*b*). If the parameter δ_2 is genuinely non-zero, it has to be understood in terms of a high-order harmonic displacive modulation of this *Imam* average structure. It is also worth noting that the O-atom array shown in Fig. 2(*b*) is very similar to the O-atom array of the α-PbO_2 structure type when projected down its [010] zone axis. For the two oxygen arrays to be made identical, however, we would require alternate columns of O atoms (along $\mathbf{a}_O$) in Fig. 2(*b*) to move up and down the $\mathbf{c}_O$ axis by exactly $\frac{1}{8}\mathbf{c}_O$ and a modulation wavevector of $\mathbf{a}_O^*$. (A similar modulation does in fact occur in this system as will be shown below. The modulation wavevector, however, is $\sim\frac{1}{2}\mathbf{a}_O^*$ rather than $\mathbf{a}_O^*$.) The relationship of the parent fluorite O-atom array to this *Cmmm*, $a_O = [x/(2+1)]a_M = \frac{8}{17}a_M$, $b_O = b_M$, $c_O = c_M$ averaged O-atom array is clear from Fig. 2(*b*), *i.e.* the parent fluorite O-atom array transforms into the *Cmmm* O-atom array *via* sheets of O atoms perpendicular to $\mathbf{b}_O$ moving $+\frac{1}{4}\mathbf{a}_O$ and $-\frac{1}{4}\mathbf{a}_O$ alternatively. Bravais-lattice-allowed O-atom subcell reflections include $(200)_O^*$, $(020)_O^*$, $(002)_O^*$, $(011)_O^*$, $(110)_O^*$ ... or $(\frac{34}{8}00)_M^*$, $(020)_M^*$, $(002)_M^*$, $(011)_M^*$, $(\frac{17}{8}10)_M^*$ if written in terms of the metal-atom subcell reciprocal lattice.

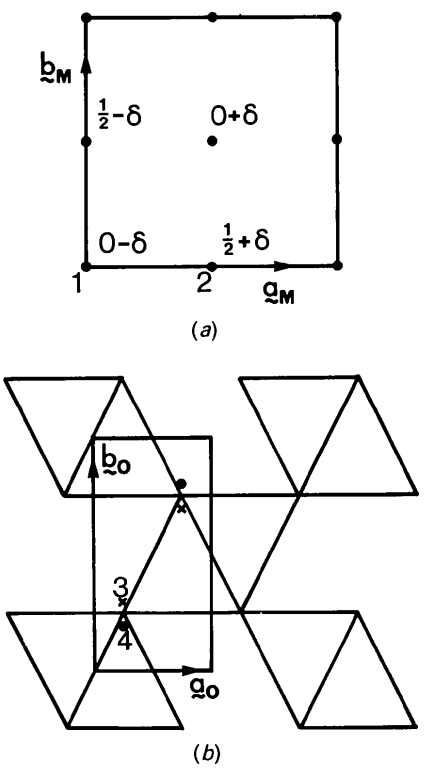

Fig. 2. (*a*) The *Amma*, $a_M = 5{\cdot}11$, $b_M = 4{\cdot}93$, $c_M = 5{\cdot}27$ Å parent metal-atom subcell obtained from the Galy–Roth structure refinement of $Nb_2Zr_6O_{17}$. The parameter δ is equal to 0·0394. The two metal-atom sites per primitive unit cell are labelled 1 and 2 respectively. (*b*) The *Ima*2, $a_O = \frac{8}{17}a_M = 2{\cdot}405$, $b_O = b_M = 4{\cdot}93$, $c_O = c_M = 5{\cdot}27$ Å, average O-atom subcell obtained from the Galy–Roth refinement. The two O-atom sites per primitive unit cell are labelled 3 and 4 respectively. Their fractional coordinates are given by $\frac{1}{4}$, $\frac{1}{4}+\delta_1$, $\frac{1}{4}+\delta_2$ and $\frac{1}{4}$, $\frac{1}{4}-\delta_1$, $\frac{1}{4}+\delta_2$. According to Galy & Roth, $\delta_1 = 0{\cdot}0233$ and $\delta_2 = 0{\cdot}0081$. The parent *Imam* O-atom subcell corresponds to setting δ_2 equal to zero.

3. Modulation of the parent metal and oxygen subcells

Having defined the parent metal and oxygen subcells, it is now necessary to allow both subcells to respond to the presence of the other. This response, or relaxation, takes the form of compositional and displacive modulation characterized by appropriate compositional and displacement eigenvectors and by modulation wavevectors which are harmonics of primary-modulation wavevectors $\mathbf{q}$ reflecting the difference between the reciprocal-lattice vectors of the parent metal and oxygen subcells.

3.1. *Primary-modulation wavevectors*

The primary-modulation wavevector characteristic of the metal sublattice is given by $\mathbf{q}_M = (110)_O^* - (200)_M^* = \mathbf{b}_M^* + \frac{1}{8}\mathbf{a}_M^*$ [$= \mathbf{b}_M^* + (1/x)\mathbf{a}_M^*$ in the general case] whilst that characteristic of the oxygen sublattice is given by $\mathbf{q}_O = \mathbf{a}_M^* = (111)_M^* - (011)_O^* = \frac{8}{17}\mathbf{a}_O^*$ {$= [x/(2x+1)]\mathbf{a}_O^*$ in the general case}. For $x = 8$, $\mathbf{q}_O = 8\mathbf{q}_M - 8\mathbf{b}_M^*$, *i.e.* $\mathbf{q}_O$ can be described as a higher-order harmonic of $\mathbf{q}_M$. For general x, however, this is not the case. The primary-modulation wavevectors characteristic of the two sublattices have to be chosen so as to be consistent with the Bravais classes (de Wolff, Janssen & Janner, 1981) of the other. Thus the reflection condition characteristic of the Bravais class of the metal sublattice, *i.e.* $F(h,k,l,m)_M^* = 0$ unless $k + l = 2n$, must be equivalent to the reflection condition characteristic of the Bravais class of the oxygen sublattice, *i.e.* $F(h',k',l',m')_O^* = 0$ unless $h' + k' + l' = 2n$, when the reciprocal-lattice vectors of one subcell are expressed in terms of the other. Thus $(h,k,l,m)_M^* = h\mathbf{a}_M^* + k\mathbf{b}_M^* + l\mathbf{c}_M^* + (m/x)\mathbf{a}_M^* + m\mathbf{b}_M^* \equiv m\mathbf{a}_O^* + (k+m)\mathbf{b}_O^* + l\mathbf{c}_O^* + (h-2m)\mathbf{a}_M^*$. That $F(h',k',l',m')_O^* = 0$ unless $h' + k' + l' = 2n$ is thus

equivalent to requiring that $k + l = 2n$, the Bravais class requiremcnt of the metal sublattice.

3.2. *Characteristic extinction conditions and superspace-group symmetry*

The superspace-group symmetry of the metal sublattice (and indeed of the whole composite modulated structure) implied by the Galy & Roth (1973) structure refinement is $M{:}Amm2{:}-1s-1$ (de Wolff *et al.*, 1981). The corresponding characteristic extinction conditions are as follows: $F(h,k,l,m)^*_M = 0$ unless $k + l = 2n$ (see Fig. 1*a*) and $F(h,k,l,-k)^*_M = 0$ unless $k = 2n$ (see Fig. 1*b*). Similarly, the superspace-group symmetry of the oxygen sublattice implied by the Galy & Roth (1973) structure refinement is $P{:}Ima2{:}-11-1$. The corresponding characteristic extinction conditions are as follows: $F(h,k,l,m)^*_O = 0$ unless $h + k + l = 2n$ and $F(h,0,l,m)^*_O = 0$ unless h, $l = 2n$. They give rise to the same extinction conditions as the metal sublattice when the oxygen subcell reciprocal-lattice vectors are expressed in terms of those of the metal-atom subcell.

The number of free structural parameters which have to be refined using the above superspace-group symmetry or symmetries is formally the same as that refined by Galy & Roth, as indeed has to be the case. However, as pointed out recently by Pérez-Mato *et al.* (1987), the number of effective structural parameters to be refined decreases when some of the higher-order harmonic modulations can be neglected for whatever reason. The observed condition, for all values of x, that $F(h,k,0,m)^*_M = 0$ unless $h = 2n$ (see Fig. 1*d*) requires that the correct superspace-group symmetry describing both the metal sublattice and the total composite structure has to be increased to $M{:}Amma{:}-1s1$ from $M{:}Amm2{:}-1s-1$ while the correct superspace-group symmetry describing the oxygen sublattice has to be increased to $P{:}Imam{:}-11s$ from $P{:}Ima2{:}-11-1$. Such an increase in superspace-group symmetry effectively cuts the number of free structural parameters in half. If the condition $F(h,k,0,m)^*_M = 0$ unless $h = 2n + 1$ had held, then the correct composite superspace-group symmetry would have been $M{:}Amma{:}-1ss$ rather than $M{:}Amma{:}-1s1$. Note, however, that $(h,k,0,8+m)^*_M \equiv (h+1,k+8,0,m)^*_M$ for x exactly equal to 8. Thus the condition that $F(h,k,0,m)^*_M = 0$ unless $h = 2n$ no longer formally exists for x exactly equal to 8. Thus, at least formally, no extinction condition now exists and, hence, reciprocal space is suddenly compatible with both the above superspace-group symmetries. The resultant composite superspace-group symmetry is $M{:}Amm2{:}-1s-1$. The reason one can still experimentally distinguish $M{:}Amma{:}-1s1$ from $M{:}Amma{:}-1ss$, even for x exactly equal to 8, is that the intensity of the various satellite reflections drops off rapidly with increasing harmonic order. Thus third- and fourth-order harmonics are barely visible in Fig. 1. Indeed no harmonics of higher order than second could ever be detected in X-ray powder patterns (Thompson *et al.*, 1990).

3.3. *Modulation of the parent metal subcell*

Given an unmodulated parent metal subcell of *Amma*, the little co-group (see Bradley & Cracknell, 1972) of the primary-modulation wavevector $\mathbf{q}_M = \mathbf{b}^*_M + \frac{1}{8}\mathbf{a}^*_M$ [$= \mathbf{b}^*_M + (1/x)\mathbf{a}^*_M$ in the general case] and all its higher-order harmonics $m\mathbf{q}$ is given by $\{E, C_{2x}, \sigma_y, \sigma_z\}$. The corresponding multiplication table is given by:

	E	C_{2x}	σ_y	σ_z
R_1	+1	+1	+1	+1
R_2	+1	+1	−1	−1
R_3	+1	−1	+1	−1
R_4	+1	−1	−1	+1

The observed composite superspace-group symmetry of $M{:}Amma{:}-1s1$ requires that the modulations associated with all odd-order harmonics transform with R_4 symmetry whereas all even-order harmonics transform with R_1 symmetry. The lower composite superspace-group symmetry of $M{:}Amm2{:}-1s-1$ allows the modulations associated with all odd-order harmonics to transform with R_2 as well as R_4 symmetry and the modulations associated with all even-order harmonics to transform with R_3 as well as R_1 symmetry. There are two metal atoms per primitive parent unit cell, labelled 1 and 2 in Fig. 2(*a*). (Because of the similarity in the atomic scattering factors of Zr and Nb for X-rays, the Galy & Roth structure refinement was unable to distinguish between Zr and Nb atoms and hence no further consideration will be given to compositional modulation in this paper.) Both R_4 and R_2 irreducible representations constrain the corresponding displacive modulations to entail only $\mathbf{b}_M$ motion whereas R_1 and R_3 irreducible representations both constrain the corresponding displacive modulations not to entail $\mathbf{b}_M$ motion. The atomic modulation functions (AMF's; see Pérez-Mato *et al.*, 1987) describing the most general possible structural deviation of these metal atoms from their underlying parent subcell, for the observed superspace-group symmetry of $M{:}Amma{:}-1s1$, can then be written in the form:

$$\begin{aligned}\mathbf{U}_1(\mathbf{T}) = \mathbf{a}_M\{&\varepsilon_x(2\mathbf{q}_M;R_1)\cos(4\pi\mathbf{q}_M.\mathbf{T} - 90°)\\ &+ \varepsilon_x(4\mathbf{q}_M;R_1)\cos(8\pi\mathbf{q}_M.\mathbf{T} - 90°) + \ldots\}\\ &+ \mathbf{b}_M\{\varepsilon_y(\mathbf{q}_M;R_4)\cos(2\pi\mathbf{q}_M.\mathbf{T} - 90°)\\ &+ \varepsilon_y(3\mathbf{q}_M;R_4)\cos(6\pi\mathbf{q}_M.\mathbf{T} - 90°) + \ldots\}\\ &+ \mathbf{c}_M\{\varepsilon_z(2\mathbf{q}_M;R_1)\cos(4\pi\mathbf{q}_M.\mathbf{T} + 0°)\\ &+ \varepsilon_z(4\mathbf{q}_M;R_1)\cos(8\pi\mathbf{q}_M.\mathbf{T} + 0°) + \ldots\}\end{aligned}$$

and

$$\mathbf{U}_2(\mathbf{T}) = \mathbf{a}_M\{\varepsilon_x(2\mathbf{q}_M;R_1)\cos(4\pi\mathbf{q}_M.[\mathbf{T}+\mathbf{a}/2]-90°) + \varepsilon_x(4\mathbf{q}_M;R_1)\cos(8\pi\mathbf{q}_M.[\mathbf{T}+\mathbf{a}/2]-90°) + \ldots\} + \mathbf{b}_M\{\varepsilon_y(\mathbf{q}_M;R_4)\cos(2\pi\mathbf{q}_M.[\mathbf{T}+\mathbf{a}/2] - 90°) + \varepsilon_y(3\mathbf{q}_M;R_4)\cos(6\pi\mathbf{q}_M.[\mathbf{T}+\mathbf{a}/2] - 90°) + \ldots\} - \mathbf{c}_M\{\varepsilon_z(2\mathbf{q}_M;R_1)\cos(4\pi\mathbf{q}_M.[\mathbf{T} + \mathbf{a}/2] + 0°) + \varepsilon_z(4\mathbf{q}_M;R_1)\cos(8\pi\mathbf{q}_M.[\mathbf{T} + \mathbf{a}/2] + 0°) + \ldots\}$$

where **T** is an allowed Bravais lattice vector of the average metal subcell and where the phases have been fixed *via* application of the superspace-group symmetry operation $\{\sigma_x|\mathbf{0},\frac{1}{2}\}$ [equivalent to the *m* in the conventional *Ima*2 space group; the superspace symmetry-operation notation is that of Pérez-Mato, Madariaga & Tello (1986) and Pérez-Mato *et al.* (1987)]. Note that for $x = 8$ only harmonics out to fourth order give independent modulation wavevectors.

The remaining structural degrees of freedom required to enable a complete fit to the Galy–Roth structure refinement (*i.e.* those structural degrees of freedom compatible with the lower composite superspace-group symmetry of M:*Amm*2:$-1s-1$ but not with the observed superspace-group symmetry of M:*Amma*:$-1s1$) can be written in the form:

$$\Delta\mathbf{U}_1(\mathbf{T}) = \mathbf{a}_M\{\varepsilon_x(2\mathbf{q}_M;R_3)\cos(4\pi\mathbf{q}_M.\mathbf{T}-90°) + \varepsilon_x(4\mathbf{q}_M;R_3)\cos(8\pi\mathbf{q}_M.\mathbf{T}-90°)+\ldots\} + \mathbf{b}_M\{\varepsilon_y(\mathbf{q}_M;R_2)\cos(2\pi\mathbf{q}_M.\mathbf{T}-90°) + \varepsilon_y(3\mathbf{q}_M;R_2)\cos(6\pi\mathbf{q}_M.\mathbf{T}-90°)+\ldots\} + \mathbf{c}_M\{\varepsilon_z(2\mathbf{q}_M;R_3)\cos(4\pi\mathbf{q}_M.\mathbf{T}+0°) + \varepsilon_z(4\mathbf{q}_M;R_3)\cos(8\pi\mathbf{q}_M.\mathbf{T}+0°)+\ldots\}$$

and

$$\Delta\mathbf{U}_2(\mathbf{T}) = -\mathbf{a}_M\{\varepsilon_x(2\mathbf{q}_M;R_3)\cos(4\pi\mathbf{q}_M.[\mathbf{T}+\mathbf{a}/2]-90°) + \varepsilon_x(4\mathbf{q}_M;R_3)\cos(8\pi\mathbf{q}_M.[\mathbf{T}+\mathbf{a}/2]-90°) + \ldots\} - \mathbf{b}_M\{\varepsilon_y(\mathbf{q}_M;R_2)\cos(2\pi\mathbf{q}_M.[\mathbf{T}+\mathbf{a}/2] - 90°) + \varepsilon_y(3\mathbf{q}_M;R_2)\cos(6\pi\mathbf{q}_M.[\mathbf{T}+\mathbf{a}/2] - 90°) + \ldots\} + \mathbf{c}_M\{\varepsilon_z(2\mathbf{q}_M;R_3)\cos(4\pi\mathbf{q}_M.[\mathbf{T} + \mathbf{a}/2] + 0°) + \varepsilon_z(4\mathbf{q}_M;R_3)\cos(8\pi\mathbf{q}_M.[\mathbf{T} + \mathbf{a}/2] + 0°) + \ldots\}$$

The values of the above parameters corresponding to the Galy–Roth structure refinement are as follows:

$\varepsilon_x(2\mathbf{q}_M;R_1) = 0{\cdot}0244$, $\varepsilon_x(4\mathbf{q}_M;R_1) - \varepsilon_x(4\mathbf{q}_M;R_3) = 0{\cdot}0014$;

$\varepsilon_y(\mathbf{q}_M;R_4) = -0{\cdot}0185$, $\varepsilon_y(3\mathbf{q}_M;R_4) = -0{\cdot}0053$;

$\varepsilon_z(2\mathbf{q}_M;R_1) = -0{\cdot}0011$, $\varepsilon_z(4\mathbf{q}_M;R_1) + \varepsilon_z(4\mathbf{q}_M;R_3) = -0{\cdot}0046$.

$\varepsilon_x(2\mathbf{q}_M;R_3) = -0{\cdot}0020$, $\varepsilon_y(\mathbf{q}_M;R_2) = 0{\cdot}0012$,

$\varepsilon_y(3\mathbf{q}_M;R_2) = 0{\cdot}0031$, $\varepsilon_z(2\mathbf{q}_M;R_3) = -0{\cdot}0034$.

The extinction condition $F(h,k,0,m)^*_M = 0$ unless $h = 2n$ (see Fig. 1*d*) constrains the latter four parameters as well as $\varepsilon_x(4\mathbf{q}_M;R_3)$ and $\varepsilon_z(4\mathbf{q}_M;R_3)$ to be zero. The conventional three-dimensional space group of *Ima*2, however, applies no such constraint. Nevertheless, they all appear to have refined to small values. If we set these six parameters equal to zero the residual modulation functions along the **a** and **b** directions appear quite reasonable, *i.e.* they are much larger than the corresponding deviation functions ΔU_{1x} and ΔU_{1y}. Such is not the case, however, along the **c** direction. According to Galy & Roth, U_{1x} is an almost purely sinusoidal function of **q.T** whereas U_{1y} is a rather more anharmonic function of **q.T**. U_{1z} *versus* **q.T** is not really very plausible. The magnitude

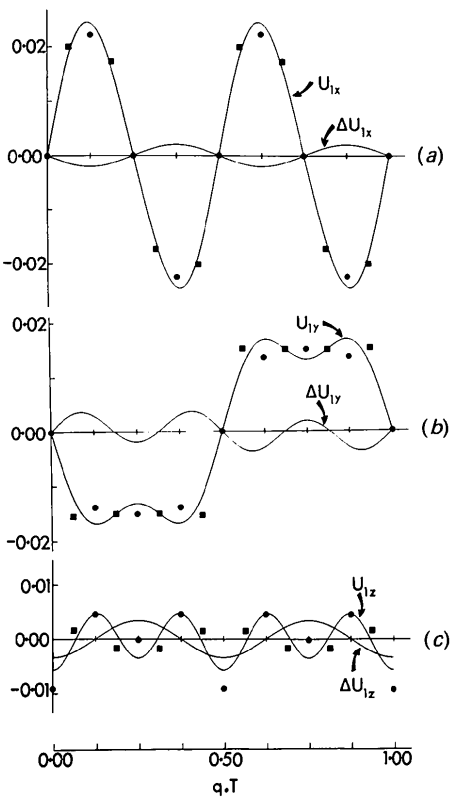

Fig. 3. Plots of (*a*) U_{1x} *versus* **q.T**, (*b*) U_{1y} *versus* **q.T** and (*c*) U_{1z} *versus* **q.T**. The corresponding deviation functions (*a*) ΔU_{1x}, (*b*) ΔU_{1y} and (*c*) ΔU_{1z}, representing the difference between the Galy–Roth modulation functions and the residual modulation functions, are also shown. The circles represent the eight independent points of each of these AMF's sampled by this particular member of the solid-solution series. The extra eight points on each of the AMF's (labelled by the squares) are derived from the shifts of metal atom 2. The amplitude of the deviation-function fluctuations gives a measure of the extent of uncertainty which should be ascribed to the corresponding residual functions or AMF's. The size of the circles and squares represents the errors quoted in the original structure refinement.

of the shifts involved, however, are very small. Fig. 3 shows plots of (*a*) U_{1x} *versus* **q.T**, (*b*) U_{1y} *versus* **q.T** and (*c*) U_{1z} versus **q.T** calculated using the above residual parameters. The corresponding deviation functions (*a*) ΔU_{1x}, (*b*) ΔU_{1y} and (*c*) ΔU_{1z}, representing the difference between the Galy–Roth modulation functions and these residual modulation functions, are also shown in Fig. 3. The circles represent the eight independent points of each of these AMF's sampled by this particular member of the solid-solution series. Note, however, that $U_{2x}(\mathbf{q.T}) \equiv U_{1x}(\mathbf{q.T} + \frac{1}{16})$, $U_{2y}(\mathbf{q.T}) \equiv U_{1y}(\mathbf{q.T} + \frac{1}{16})$ and $U_{2z}(\mathbf{q.T}) \equiv -U_{1z}(\mathbf{q.T} + \frac{1}{16})$. The extra eight points on each of the AMF's in Fig. 3 (labelled by the squares) are thus derived from the shifts of metal atom 2. In general, *i.e.* for irrational x, all possible values will be sampled. The amplitude of the deviation-function fluctuations gives a measure of the extent of uncertainty which should be ascribed to the corresponding residual functions or AMF's. (Note that the size of the circles and squares in Fig. 3 represents the errors quoted in the original structure refinement.) It seems unlikely that these AMF's would vary much with x. However this could only be determined by further structure refinements at other values of x.

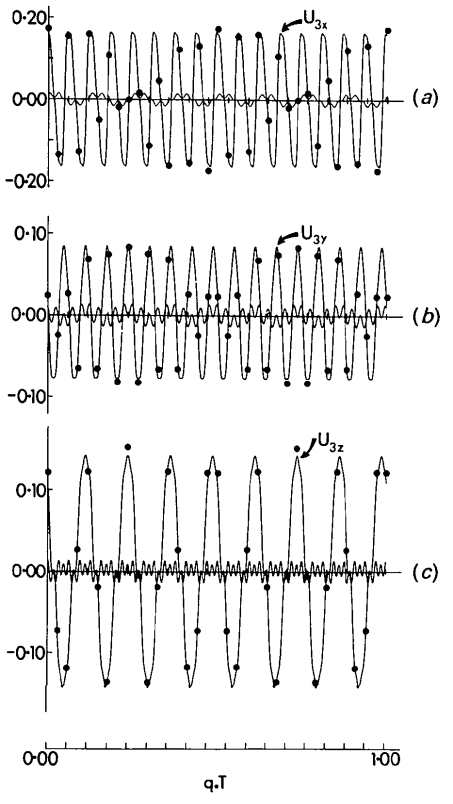

Fig. 4. Plots of (*a*) U_{3x} *versus* **q.T**, (*b*) U_{3y} *versus* **q.T** and (*c*) U_{3z} *versus* **q.T**. The corresponding deviation functions are also shown. Again the amplitude of the deviation-function fluctuations gives a measure of the extent of uncertainty which should be ascribed to the corresponding residual functions or AMF's. The circles represent the 34 independent points of each of these AMF's sampled by this particular member of the solid-solution series.

3.4. *Modulation of the average oxygen subcell*

Given an unmodulated parent oxygen subcell of *Imam*, the little co-group of the primary-modulation wavevector $\mathbf{q}_O = \mathbf{a}^*_M$ {$=[x/(2x+1)]\mathbf{a}^*_O$ in the general case} and all its higher-order harmonics $m\mathbf{q}$ is also given by $\{E,C_{2x},\sigma_y,\sigma_z\}$. The corresponding multiplication table is the same as that given above in §3.3. The above superspace group requires that the modulations associated with all odd-order harmonics transform with R_3 symmetry whereas all even-order harmonics transform with R_1 symmetry. There are two atoms per primitive parent unit cell, labelled 3 and 4 in Fig. 2(*b*).

An R_3 irreducible representation constrains the corresponding displacive modulation to entail only $\mathbf{c}_O$ motion whereas an R_1 irreducible representation constrains the corresponding displacive modulation *not* to entail c_O motion. The AMF's (see Pérez-Mato *et al.*, 1987) describing the most general possible structural deviation of these O atoms from their underlying average subcell, for the observed superspace-group symmetry of *M*:*Amma*:$-1s1$, can then be written in the form:

$$\begin{aligned}U_{3,4}(\mathbf{T}_O) = a_O\{&\varepsilon_x(2\mathbf{q}_O;R_1)\cos(4\pi\mathbf{q}_O.[\mathbf{T}_O + \mathbf{a}_O/4] - 90°)\\ &+ \varepsilon_x(4\mathbf{q}_O;R_1)\cos(8\pi\mathbf{q}_O.[\mathbf{T}_O + \mathbf{a}_O/4] - 90°)\\ &+ \ldots\} \pm \mathbf{b}_O\{\varepsilon_y(2\mathbf{q}_O;R_1)\cos(4\pi\mathbf{q}_O.[\mathbf{T}_O\\ &+ \mathbf{a}_O/4]) + \varepsilon_y(4\mathbf{q}_O;R_1)\cos(8\pi\mathbf{q}_O.[\mathbf{T}_O\\ &+ \mathbf{a}_O/4]) + \ldots\}\\ &+ \mathbf{c}_O\{\varepsilon_z(\mathbf{q}_O;R_3)\cos(2\pi\mathbf{q}_O.[\mathbf{T}_O + \mathbf{a}_O/4])\\ &+ \varepsilon_z(3\mathbf{q}_O;R_3)\cos(6\pi\mathbf{q}_O.[\mathbf{T}_O + \mathbf{a}_O/4]) + \ldots\},\end{aligned}$$

where $\mathbf{T}_O$ is an allowed Bravais lattice vector of the average O-atom subcell, the $\pm$ sign corresponds to O atoms 3 and 4 respectively, and the phases are fixed by the superspace-group symmetry operation $\{\sigma_x|\frac{1}{2}\mathbf{a}_O, -\mathbf{q}_O.\frac{1}{2}\mathbf{a}_O\}$ (equivalent to the m in the conventional *Ima*2 space group). The remaining structural degrees of freedom required to enable a complete fit to the Galy–Roth structure refinement can be written in the form:

$$\begin{aligned}\Delta\mathbf{U}_{3,4}(\mathbf{T}_O) = \mathbf{a}_O\{&\varepsilon_x(\mathbf{q}_O;R_1)\cos(2\pi\mathbf{q}_O.[\mathbf{T}_O + \mathbf{a}_O/4] - 90°)\\ &+ \varepsilon_x(3\mathbf{q}_O;R_1)\cos(6\pi\mathbf{q}_O.[\mathbf{T}_O + \mathbf{a}_O/4]\\ &- 90°) + \ldots\}\\ &\pm \mathbf{b}_O\{\varepsilon_y(\mathbf{q}_O;R_1)\cos(2\pi\mathbf{q}_O.[\mathbf{T}_O + \mathbf{a}_O/4])\\ &+ \varepsilon_y(3\mathbf{q}_O;R_1)\cos(6\pi\mathbf{q}_O.[\mathbf{T}_O + \mathbf{a}_O/4]) + \ldots\}\\ &+ \mathbf{c}_O\{\varepsilon_z(2\mathbf{q}_O;R_3)\cos(4\pi\mathbf{q}_O.[\mathbf{T}_O + \mathbf{a}_O/4])\\ &+ \varepsilon_z(4\mathbf{q}_O;R_3)\cos(8\pi\mathbf{q}_O.[\mathbf{T}_O + \mathbf{a}_O/4]) + \ldots\}\end{aligned}$$

The values of the above parameters corresponding to the Galy–Roth structure refinement are as follows:

$$\varepsilon_x(2\mathbf{q}_O;R_1) = 0{\cdot}1692,\ \varepsilon_x(4\mathbf{q}_O;R_1) = 0{\cdot}0354,$$
$$\varepsilon_x(6\mathbf{q}_O;R_1) = 0{\cdot}0105,\ \varepsilon_x(8\mathbf{q}_O;R_1) = 0{\cdot}0143;$$
$$\varepsilon_y(2\mathbf{q}_O;R_1) = 0{\cdot}0843,\ \varepsilon_y(4\mathbf{q}_O;R_1) = -0{\cdot}0007,$$
$$\varepsilon_y(6\mathbf{q}_O;R_1) = -0{\cdot}0031,\ \varepsilon_y(8\mathbf{q}_O;R_1) = 0{\cdot}0048;$$
$$\varepsilon_z(\mathbf{q}_O;R_3) = 0{\cdot}1361,\ \varepsilon_z(3\mathbf{q}_O;R_3) = 0{\cdot}0128,$$
$$\varepsilon_z(5\mathbf{q}_O;R_3) = -0{\cdot}0141,\ \varepsilon_z(7\mathbf{q}_O;R_3) = 0{\cdot}0083,$$
$$\varepsilon_z(17\mathbf{q}_O \equiv \mathbf{0};R_1) = 0{\cdot}0081;$$
$$\varepsilon_x(\mathbf{q}_O;R_1) = 0{\cdot}0116,\ \varepsilon_x(3\mathbf{q}_O;R_1) = 0{\cdot}0034,$$
$$\varepsilon_x(5\mathbf{q}_O;R_1) = -0{\cdot}0050,\ \varepsilon_x(7\mathbf{q}_O;R_1) = -0{\cdot}0006;$$
$$\varepsilon_y(\mathbf{q}_O;R_1) = 0{\cdot}0055,\ \varepsilon_y(3\mathbf{q}_O;R_1) = 0{\cdot}0027,$$
$$\varepsilon_y(5\mathbf{q}_O;R_1) = -0{\cdot}0094,\ \varepsilon_y(7\mathbf{q}_O;R_1) = -0{\cdot}0005;$$
$$\varepsilon_z(2\mathbf{q}_O;R_1) = 0{\cdot}0054,\ \varepsilon_z(4\mathbf{q}_O;R_3) = -0{\cdot}0046,$$
$$\varepsilon_z(6\mathbf{q}_O;R_1) = -0{\cdot}0004,\ \varepsilon_z(8\mathbf{q}_O;R_3) = 0{\cdot}0095.$$

The extinction condition $F(h,k,0,m)^*_M = 0$ unless $h = 2n$ (Fig. 1*d*) constrains the latter 12 parameters to be zero. The conventional three-dimensional space group of *Ima*2, however, applies no such constraint. Nevertheless, again they all appear to have refined to quite small values, generally less than 0·01. This then is the level of accuracy to which we should trust the residual parameters. If we set these 12 parameters equal to zero the residual modulation functions along the $\mathbf{a}_O$, $\mathbf{b}_O$ and $\mathbf{c}_O$ directions are large (much larger than the metal-atom shifts *i.e.* $\simeq \pm 0{\cdot}4$ Å along $\mathbf{a}_O$, $\mathbf{b}_O$ and $\simeq \pm 0{\cdot}7$ Å along $\mathbf{c}_O$) and apparently fairly sinusoidal, although there is clearly a need for further structure refinement using a modulated structure, or superspace-group, approach. Fig. 4 shows plots of (*a*) U_{3x} *versus* $\mathbf{q}.\mathbf{T}$, (*b*) U_{3y} *versus* $\mathbf{q}.\mathbf{T}$ and (*c*) U_{3z} *versus* $\mathbf{q}.\mathbf{T}$ calculated using the above residual parameters. The corresponding deviation functions are also shown. Again the amplitude of the deviation-function fluctuations gives a measure of the extent of uncertainty which should be ascribed to the corresponding residual functions or AMF's. The circles represent the 34 independent points of each of these AMF's sampled by this particular member of the solid-solution series. In general, *i.e.* for irrational

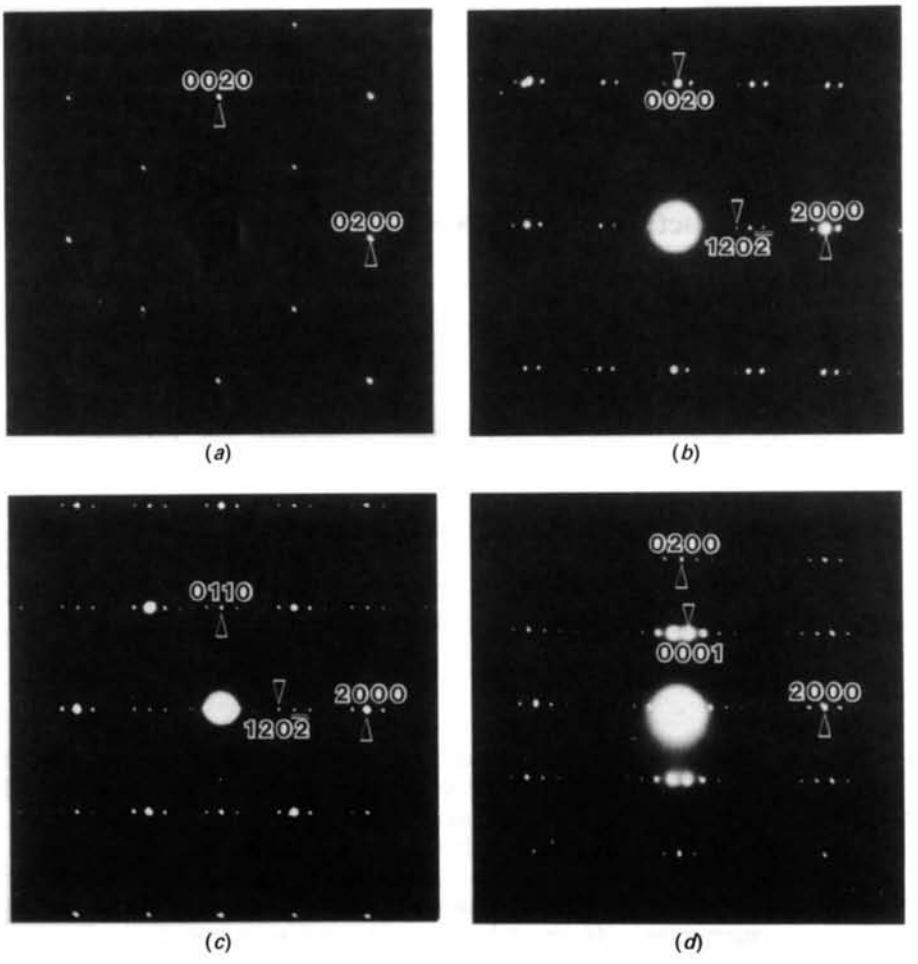

Fig. 5. (*a*) $[100]_M$, (*b*) $[010]_M$, (*c*) $[0\bar{1}1]_M$ and (*d*) $[001]_M$ zone-axis selected area electron diffraction patterns (SADP's) typical of $Nb_2Zr_{x-2}O_{2x+1}$ (x = 7·1–10·3). Note the very slight canting of the satellite reflections away from the $\mathbf{a}^*_M$ direction in the latter three SADP's.

x, all possible values will be sampled. It seems unlikely that these AMF's would vary much with x. However this could only be determined by further structure refinements at other values of x.

4. Complications

The very recent observation (Thompson *et al.*, 1990) that the true value is $\mathbf{q} = (1/x)\mathbf{a}_M^* + (1-\varepsilon)\mathbf{b}_M^* + \delta\mathbf{c}_M^*$ (with ε and δ very small but definitely non-zero across the whole solid-solution field; see Fig. 5) means that the composite superspace group of *M*:*Amma*:−1*s*1 given above cannot strictly be correct (in fact the implied triclinicity of the oxygen subcell strictly reduces the composite superspace-group symmetry to the trivial *P*:*P*1:1). In terms of the modulation functions given in §3.3 and 3.4 above, such a symmetry reduction allows shifts along **a**, **b** and **c** to exist for each modulation harmonic. In practice, however, the extinction conditions implied by a superspace-group symmetry of *M*:*Amma*:−1*s*1 are clearly still valid *i.e.* the amplitudes of these extra symmetry-compatible distortions must be vanishingly small. Structure-factor expressions, such as that given in Pérez-Mato *et al.* (1986) for example, are compatible with this interpretation provided ε and δ are small. Hence the expressions given above for $\mathbf{U}_1(\mathbf{T})$, $\mathbf{U}_2(\mathbf{T})$ and $\mathbf{U}_{3,4}(\mathbf{T}_O)$ remain valid except that $\mathbf{q}_M$ and $\mathbf{q}_O$ have to be very slightly altered to allow for incommensurability along **b** and **c** as well as along **a**. Similarly, the parent O-atom subcell shown in Fig. 2(*b*) must be very slightly strained to be compatible with experimental observation.

References

BRADLEY, C. J. & CRACKNELL, A. P. (1972). *The Mathematical Theory of Symmetry in Solids*. Oxford: Clarendon Press.

GALY, J. & ROTH, R. S. (1973). *J. Solid State Chem.* **7**, 277–285.

JANNER, A. & JANSSEN, T. (1980). *Acta Cryst.* A**36**, 408–415.

PÉREZ-MATO, J. M., MADARIAGA, G. & TELLO, M. J. (1986). *J. Phys. C*, **19**, 2613–2622.

PÉREZ-MATO, J. M., MADARIAGA, G., ZUÑIGA, F. J. & GARCIA ARRIBAS, A. (1987). *Acta Cryst.* A**43**, 216–226.

ROTH, R. S., WARING, J. L., BROWER, W. S. & PARKER, H. S. (1972). *Solid State Chemistry, Proceedings of the 5th Materials Research Symposium*, NBS Special Publication No. 364, edited by R. S. ROTH & J. S. SCHNEIDER, pp. 183–195. Washington, DC: National Bureau of Standards.

THOMPSON, J. G., WITHERS, R. L., SELLAR, J., BARLOW, P. J. & HYDE, B. G. (1990). *J. Solid State Chem.* **88**, 465–475.

WOLFF, P. M. DE, (1974). *Acta Cryst.* A**30**, 777–785.

WOLFF, P. M. DE, (1988). *Z. Kristallogr.* **185**, 67.

WOLFF, P. M. DE, JANSSEN, T. & JANNER, A. (1981). *Acta Cryst.* A**37**, 625–636.

Acta Cryst. (1991). B**47**, 174–180

Revised Structure of Bi_3TiNbO_9

BY J. G. THOMPSON

Research School of Chemistry, Australian National University, GPO Box 4, *Canberra, ACT* 2601, *Australia*

A. D. RAE

School of Chemistry, University of New South Wales, PO Box 1, *Kensington, NSW* 2033, *Australia*

R. L. WITHERS

Research School of Chemistry, Australian National University, GPO Box 4, *Canberra, ACT* 2601, *Australia*

AND D. C. CRAIG

School of Chemistry, University of New South Wales, PO Box 1, *Kensington, NSW* 2033, *Australia*

(*Received* 10 *July* 1990; *accepted* 28 *September* 1990)

Abstract

The displacive ferroelectric Bi_3TiNbO_9 [$M_r = 911{\cdot}7$, orthorhombic, $A2_1am$, $a = 5{\cdot}4398$ (7), $b = 5{\cdot}3941$ (7), $c = 25{\cdot}099$ (5) Å, $D_x = 8{\cdot}223$ g cm^{-3}, $Z = 4$, Mo $K\alpha$, $\lambda = 0{\cdot}7107$ Å, $\mu = 737{\cdot}6$ cm^{-1}, $F(000) = 1535{\cdot}3$] is described at room temperature as a commensurate modulation of an *Fmmm* parent structure. Displacive modes of *F*2*mm*, *Amam* and *Abam* symmetry are all substantial and reduce the symmetry to $A2_1am$. A final value of 0·0295 for $R_1 = \sum_{\mathbf{h}}||F_{obs}(\mathbf{h})| - |F_{calc}(\mathbf{h})||/\sum_{\mathbf{h}}|F_{obs}(\mathbf{h})|$ was obtained for the 1386 unmerged data used for refinement. The modes of *Amam* and *Abam* symmetry were essentially the same

0108-7681/91/020174-07$03.00